ELSEVIER

Spectrochimica Acta Part A 55 (1999) 999–1010

SPECTROCHIMICA ACTA
PART A

Solvent effects on vibrational spectrum of hydrogen-bonded complex PhOH···H_2O. An ab initio study

Yordanka Dimitrova *

Institute of Organic Chemistry, Bulgarian Academy of Sciences, Bl. 9, 1113, Sofia, Bulgaria

Received 9 February 1998; accepted 29 July 1998

Abstract

The vibrational features characterising the hydrogen-bonded interaction between PhOH and H_2O have been studied. The vibrational spectra for free and complexed PhOH and H_2O have been predicted by ab initio calculations at different levels: 3–21G/SCF, 6–31G/SCF and 6-31G/MP2. The changes in the vibrational characteristics (vibrational frequencies, infrared intensities and Raman activities) upon hydrogen bonding have been estimated. It was established that the most sensitive to the complexation is the stretching O–H vibration of the phenol site. In agreement with the experiment, its vibrational frequency is shifted to lower wavenumbers. The magnitude of the wavenumber shift is indicative of a relatively strong OH···H hydrogen-bonded interaction. The ab initio calculations at different levels predict an increase of the IR intensity up to 50 times and of the Raman activity up to four times. The remaining vibrations (stretching, bending and torsion) are less sensitive to the hydrogen bonding. Their vibrational characteristics are changed to a less extent.

Keywords: Ab initio calculations; Hydrogen-bonded complex; Vibrational spectra

1. Introduction

The hydogen-bonded phenol complexes with simple solvent molecules are important models for investigation of H-bonding and proton transfer in proteins and nucleic acids.

In recent years, the experimental studies on vibrational spectra of phenol and clusters with water, methanol, and ammonia have gained much interest [1–10]. The vibrational spectra in the ground state of the complexes are of particular importance, in order to examine the complex structure, because vibrational frequencies are determined by the force field which is directly related to the structure. It is anticipated that the normal modes of phenol which involve stretching, bending, and torsion vibrations of the OH group undergo substantial changes in the frequencies due to hydrogen bonding. The frequency shifts of these modes give direct information on the H-bond interaction. Especially, the frequency change of the phenolic OH stretching vibration closely correlates with the H-bond strength which depends on the basicity of the acceptor. The observations of vibrational spectra of acceptors are

* Fax: +359-2-931-0018.
E-mail address: dyor@bgearn.acad.bg (Y. Dimitrova)

1386-1425/99/$ - see front matter
PII: S1386-1425(98)00243-1

quite important to characterise their coordination in the complex.

Phenol (PhOH) is the simplest aromatic acid as it is well known, in aqueous solution the molecule is hydrated. The study of the phenol-water complex PhOH···$(H_2O)n$ is a natural first step for understanding molecular interactions in organic acids. In recent cluster chemistry IR spectroscopy has been extensively used for obtaining information on cluster structures which are otherwise difficult to be determined directly. Recently, the Mikami and Ebata group succeeded in observing the IR spectra of PhOH···$(H_2O)_n$ ($n \leq 4$) [11,12].

The combination of ab initio calculations and experimental data leads to a better knowledge of the nature of hydrogen bonding. Burgi et al. [13] determined a ring structure of PhOH···$(H_2O)_3$ using the 6–31G**/SCF basis set, and examined the intermolecular vibrations. The intermolecular and intramolecular vibrations of a ring structure of PhOH···$(H_2O)_2$ have been investigated by ab initio calculations using different basis sets [14].

It is known that hydrogen bonding leads to substantial changes in the vibrational characteristics of the stretching vibrations for the monomer bonds involved in the hydrogen bonding. In our previous studies [15–17] the shifts in the vibrational frequencies of formaldehyde and proton donors of varying strengths: N≡COH, NH=CHOH and H_2O upon formation of the hydrogen-bonded complexes have been predicted using ab initio calculations at different basis sets. The predicted frequency shifts are in good agreement with the experimental shifts. It was established that the stretching frequencies for monomer bonds involved in hydrogen bonding are shifted to lower frequency corresponding to bond weakening. The remaining frequencies are either unchanged, or shifted to higher frequency.

The aim of the present study is to investigate the solvent shifts in the vibrational characteristics (vibrational frequencies, infrared intensities and Raman activities) upon hydrogen bonding for the hydrogen-bonded complex PhOH···H_2O using ab initio calculations at different levels. The first step in our study is to optimise the geometric parameters for the monomers (PhOH and H_2O) and for the complex PhOH···H_2O at different levels of ab initio MO theory: 6–31G/SCF, 6–31G/MP2, DZP/SCF and DZP/MP2. The calculated values of the geometric parameters are compared with the corresponding experimental data. The second step is to predict the vibrational characteristics (vibrational frequencies, IR intensities and Raman activities) of the monomers and of the complex by ab initio calculations at different levels: 3–21G/SCF, 6–31G/SCF and 6–31G/MP2, and finally to estimate the changes in the vibrational characteristics from monomers to a complex.

2. Results and discussion

2.1. Geometries

In a previous our study [18] the structures and stabilities of the hydrogen-bonded complexes of phenol with 1–4 water molecules have been investigated employing ab initio calculations at different levels. The most stable structures of the phenol–water complexes have been determined. The dissociation energy has been estimated employing basis set superposition correction, zero-point vibrational contribution and MP2 correlation contribution.

The object of the present study is the complex of phenol with one water molecule, which has a planar structure (see Fig. 1). For the complex studied full geometry optimization has been per-

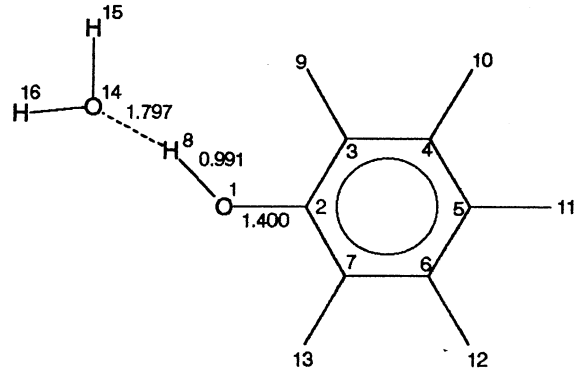

Fig. 1. Optimized structure at 6–31G/MP2 level end atomic numbering for the complex PhOH···H_2O.

Table 1
Calculated and experimental geometric parameters for free and complexed PhOH and H_2O

Parameter[a]	6–31G/SCF		6–31G/MP2		DZP/SCF		DZP/MP2		Exp[d]
	Monomer	complexation	Monomer	complexation	Monomer	complexation	Monomer	complexation	Monomers
Bond length[b]									
C_2O_1	1.377	1.365	1.415	1.401	1.353	1.345	1.376	1.366	1.364
C_3C_2	1.385	1.388	1.409	1.114	1.389	1.391	1.402	1.406	1.398
C_4C_3	1.389	1.388	1.413	1.413	1.391	1.389	1.403	1.402	1.398
C_5C_4	1.385	1.386	1.411	1.411	1.386	1.386	1.401	1.402	1.398
C_6C_5	1.391	1.391	1.415	1.415	1.392	1.392	1.404	1.404	1.398
C_7C_6	1.384	1.384	1.408	1.408	1.385	1.385	1.399	1.399	1.398
H_8O_1	0.949	0.960	0.980	0.991	0.943	0.949	0.966	0.974	0.956
H_9C_3	1.074	1.073	1.093	1.092	1.077	1.076	1.087	1.085	1.076
$H_{10}C_4$	1.073	1.073	1.091	1.091	1.075	1.076	1.085	1.085	1.076
$H_{11}C_5$	1.072	1.073	1.090	1.091	1.074	1.075	1.084	1.085	1.082
$H_{12}C_6$	1.073	1.073	1.091	1.091	1.075	1.076	1.085	1.085	1.076
$H_{13}C_7$	1.071	1.071	1.089	1.089	1.074	1.075	1.084	1.084	1.076
$O_{14}O_1$	–	2.773	–	2.781	–	2.894	–	2.807	–
$H_{15}O_{14}$	0.949	1.949	0.975	0.977	0.944	0.944	0.962	0.963	0.957[e]
$H_{16}O_{14}$	0 949	0.949	0.975	0.973	0.944	0.945	0.962	0.963	0.957
Angle[c]									
$C_3C_2O_1$	122.5	122.6	122.8	123.0	122.3	122.6	122.6	122.6	122.5
$C_4C_3C_2$	119.5	119.7	119.2	119.6	119.6	119.8	119.6	119.8	–
$C_5C_4C_3$	120.4	120.6	120.4	120.5	120.7	120.9	120.4	120.8	–
$C_6C_5C_4$	119.4	119.2	119.6	119.4	119.1	118.9	119.4	118.9	–
$C_7C_6C_5$	120.6	120.6	120.5	120.5	120.8	120.9	120.6	120.9	–
$H_8O_1C_2$	114.8	115.9	110.9	111.9	110.9	112.0	108.4	111.9	109.0
$H_9C_3C_2$	120.3	119.9	120.5	120.0	120.2	119.9	120.1	119.9	–
$H_{10}C_4C_3$	119.4	119.3	119.4	119.4	119.2	119.2	119.3	119.2	–
$H_{11}C_5C_4$	120.3	120.4	120.2	120.3	120.4	120.6	120.3	120.5	–
$H_{12}C_6C_5$	119.9	119.9	120.0	119.9	119.8	119.8	119.9	119.8	–
$H_{13}C_7C_6$	121.7	121.7	121.8	121.7	121.4	121.3	121.5	121.3	–
$O_{14}O_1C_2$	–	121.7	–	117.4	–	121.0	–	121.0	–
$H_{15}O_{14}O_1$	–	137.0	–	137.3	–	139.8	–	139.9	–
$H_{16}O_{14}O_1$	–	110.6	–	111.8	–	112.7	–	112.8	
$H_{15}O_{14}H_{16}$	111.5	112.4	109.3	110.8	106.6	107.4	104.6	107.3	104.5[e]

[a] See Fig. 1 for numbering of atoms.
[b] In angstroms.
[c] In degrees.
[d] [40]
[e] [41]

formed at different levels of ab initio MO theory: 6–31G/SCF, 6–31G/MP2, DZP/SCF and DZP/MP2. The optimum values of the geometric parameters for the monomers (PhOH and H_2O) and for the complex PhOH···H_2O are given in Table 1. The calculated values for the monomers are compared with the corresponding experimental data.

As can be seen from the results presented in Table 1, the calculated bond lengths and angles with the DZP basis set are in better agreement with the experimental data than the corresponding parameters calculated with the 6–31G basis set. The calculated bond lengths are longer than the corresponding values calculated at the SCF level. The angles, calculated at the MP2 level are

Table 2
Net atomic charges (q_i) and changes of the atomic charges (Δq_i) from monomers (PhOH and H_2O) to complex ($PhOH\cdots H_2O$) calculated at the different levels of ab initio MO theory

No[a]	Atom	6–31G**/SCF		6–31G**/MP2		DZP/SCF		DZP/MP2	
		q_i	Δq_i[b]	q_i	Δq_i[b]	q_i	Δq_i[b]	q_i	Δq_i[b]
1	O	−0.6905	−0.0348	−0.6364	−0.0599	−0.5245	−0.0201	−0.5499	−0.1016
2	C	0.3995	0.0092	0.3213	0.0080	0.4116	0.0003	0.4112	0.0659
3	C	−0.2223	−0.0024	−0.1595	−0.0073	−0.2742	0.0022	−0.2659	−0.0154
4	C	−0.1281	−0.0008	−0.1294	−0.0017	−0.0548	0.0017	−0.0610	0.0177
5	C	−0.1800	−0.0045	−0.1265	−0.0029	−0.1716	0.0082	−0.1705	−0.0400
6	C	−0.1294	0.008	−0.1303	−0.0022	−0.0508	−0.0003	−0.0567	0.0165
7	C	−0.1886	−0.0069	−0.1357	−0.0033	−0.2373	−0.0126	−0.2337	−0.0345
8	H	0.3963	0.0483	0.3837	0.0515	0.3921	0.0473	0.4079	0.0757
9	H	0.1359	−0.0028	0.0986	−0.0129	0.0905	0.0026	0.0938	0.0031
10	H	0.1431	−0.0082	0.1133	−0.0081	0.0913	−0.0062	0.0932	−0.0026
11	H	0.1400	−0.0067	0.1136	−0.0060	0.0982	−0.0050	0.0997	0.0005
12	H	0.1456	−0.0065	0.1167	−0.0029	0.0968	−0.0052	0.0987	−0.0005
13	H	0.1569	0.0048	0.1304	0.0083	0.1173	−0.0055	0.1192	0.0010
14	O	−0.6833	−0.0126	−0.6594	−0.0184	−0.7081	−0.0315	−0.7209	−0.0632
15	H	0.3510	0.0156	0.3481	0.0276	0.3591	0.0208	0.3665	0.0378
16	H	0.3541	0.0187	0.3515	0.0310	0.3608	0.0225	0.3686	0.0397

[a] See Fig. 1 for numbering of atoms.
[b] Δq_i $q_i^{complex} - q_i^{monomer}$

in better agreement with the experiment than the results at the SCF level.

It is interesting to investigate the changes in the geometric parameters from free monomers to a complex. The most sensitive to the formation of the hydrogen bond is the hydrogen-bonded OH bond (H_8O_1) and the angle $H_8O_1C_2$ The remaining geometric parameters of the monomers are either unchanged or changed with small values upon formation of the hydrogen bond.

2.2. Charge distribution

In order to determine the influence of the hydrogen bonding on the charge rearangement for the studied phenol–water complex, the Mulliken population analysis has been used in this work. The charge distribution for the monomers (PhOH and H_2O) and for the complex $PhOH\cdots H_2O$ has been evalueted by ab initio calculations at different levels: 6–31G**/SCF, 6–31G**/MP2, DZP/SCF and DZP/MP2. The calculated net atomic charges (q_i) and the changes of the atomic charges (Δq_i) from monomers to a complex are presented in Table 2.

The data for q_i and Δq_i (see Table 2) show that as a result of hydrogen bonding between PhOH and H_2O a charge rearrangement occurs. The most sensitive to the complexation are the atoms O_1 and H_8 (from PhOH), and O_{14} (from H_2O). The negativity of the oxygen atoms O_1 and O_{14} increases upon hydrogen bonding, while the hydrogen atom H_8 releases positive charge change. It can be concluded that the oxygen atoms O_1 and O_{14} act as an acceptor of electric charge in the process of the complexation. At the same time the positivity of the hydrogen atom H_8 increases.

The changes of the electric charges of the other atoms in the complex $PhOH\cdots H_2O$ are smaller or low insignificant.

2.3. Vibrational frequencies and intensities

A molecule surrounded by a small number of other molecules represents a molecular model of a solute-solvent system in condensed phase. Solvent effects in bulk systems can be used for elucidation of the structure of clusters. Since phenol is a prototype among many hydrogen-donating aro-

matics, spectroscopic studies of clusters of phenol with hydrogen-accepting molecules will contribute to the investigation of the structure of these systems.

In recent years the prediction of the vibrational characteristics (vibrational frequencies, infrared intensities and Raman activities) of the hydrogen-bonded systems by ab initio calculations at different levels [15–17,19–29] has become widely employed in order to elucidate the influence of the hydrogen bonding on the vibrational spectra of the complexes.

It is known that certain ab initio predicted values of vibrational frequencies and IR intensities are not expected to be accurate. The frequencies from calculations with larger basis sets give reasonable prediction to the experimental values, if the vibrations have small anharmonicity. Thus the combination of ab initio calculations and experimental data leads to a better knowledge of the nature of hydrogen bonding.

In order to predict the vibrational frequencies, infrared intensities and Raman activities, characterizing the interaction between PhOH and H_2O, ab initio calculations at different levels: 3–21G/SCF, 6–31G/SCF and 6–31G/MP2 have been performed for free monomers (PhOH and H_2O) and for the dimer PhOH···H_2O.

Table 3 presents a detailed description of the normal modes of phenol and water (vibrational assignment) based on the potential energy distribution (PED) obtained from the 6–31G/SCF calculations. The calculated values of the vibrational frequencies, infrared intensities and Raman activities at the 3–21G/SCF, 6–31G/SCF and 6–31G/MP2 levels for free monomers are presented in the Table 3. The calculated vibrational characteristics are compared with the corresponding experimental data [30–34]. As can be seen from the results in Table 3, the 3–21G/SCF and 6–3lG/SCF basis sets overestimate the values of the vibrational frequencies of the order of 10%. The average scale factors for the stretching, bending and torsion vibrations for the 3–2lG/SCF calculated frequencies is 0.8997, and for the 6–31G/SCF calculated frequencies is 0.8944. The calculated vibrational frequencies with the 6–31G/MP2 level are in best agreement with the experimental data. The accurate prediction of the vibrational characteristics for hydrogen-bonded complexes by extended basis sets in the MP2 level was extensively discussed recently [35,36].

For the complex of phenol with one water molecule, shown in Fig. 1, the vibrational frequencies, infrared intensities and Raman activities are predicted by ab initio calculations at 3–21G/SCF, 6–31G/SCF and 6–31G/MP2 levels. The potential energy distribution (PED), obtained from 6–31G/SCF calculations is used for a description of the normal modes. The predicted vibrational characteristics and PED's elements for the complex PhOH···H_2O are shown in Table 4. Different PED's elements obtained with the MP2 method for free and complexed PhOH and H_2O are indicated in the end of the second column of Tables 3 and 4.

As can be seen from the results for approximate description (PED) presented in Table 4, most of the intramolecular vibrations of the dimer can be correlated with normal modes of the monomers, described in Table 3. The hydrogen bond formation in the complex leads to the changes in the percentage contributions (PED's elements) of localized modes to each normal mode. In addition to the 33 and three frequencies obtained for the monomers (PhOH and H_2O) (see Table 3), there are six more intermolecular vibrations (see Table 4, modes $\nu_1 - \nu_6$), which arise from the complexation of phenol and water: the stretching O···H vibration (ν_4), the torsional vibrations (ν_1, ν_3 and ν_5) and in plane bending vibrations (ν_2 and ν_6).

The ab initio calculations predict O···H stretching vibration in the range: 177.5–189.3 cm^{-1}, with medium IR intensity. Bearing in mind, that the predicted vibrational frequencies at the 6–31G/MP2 level are in best agreement with the experimental data, we can conclude that the stretching O···H vibration appears at 189.3 cm^{-1}. The other intermolecular vibrations (modes ν_1, ν_2, ν_3, ν_5, and ν_6) are predicted at the 6–31G/MP2 level in the range 40.0–240.2 cm^{-1}.

The accuracy of ab initio prediction of the vibrational frequencies can be increased by the utilization of scaling procedures [37,38]. In order to improve the estimates of the frequency shifts

Table 3
Experimental vibrational characteristics (ν, cm^{-1}; A, km mol^{-1}) and calculated vibrational characteristics (ν, cm^{-1}; A, km mol^{-1}, R.a., A^4 amu^{-1}) at different levels of ab initio MO theory for PhOH and H_2O

Mode	Approximate description[a]	Exp[c]		3–21G/SCF			6–31G/SCF			6–31G/MP2	
	(PED)[b]	ν	A	ν	A	R.a.	ν	A	R.a.	ν	A
PhOH											
ν_1	$\tau_1(68)+\tau_3(28)$ [(a)]	244.5	–	265.3	8.4	1.9	261.5	4.1	2.2	222.7	0.1
ν_2	τOH(100)	309.2	47	315.1	187.1	5.7	323.9	212.8	4.2	307.7	181.6
ν_3	δCO(81)	403.1	5	426.9	13.5	0.6	431.8	14.7	0.5	394.6	13.1
ν_4	τ_3 (43)+τ_4(43)	408.5	0.0	482.6	0.1	0.0	475.4	0.1	0.0	399.5	0.6
ν_5	$\tau_3(50)+\gamma$CO(30)+γC_6H(11) [(b)]	502.8	26	588.3	7.2	0.0	574.8	7.8	0.0	431.6	1.8
ν_6	$\delta_1(47)+\delta_2(24)+\nu$C–O (13)	526.6	5	590.6	2.5	5.2	585.2	2.9	0.5	483.1	0.6
ν_7	$\delta_2(90)$ [(c)]	618.7	–	709.9	0.2	4.3	701.6	0.3	4.8	535.0	2.6
ν_8	$\tau_2(71)$ [(d)]	685.9	50	807.4	41.8	0.1	789.4	25.7	0.0	641.7	0.3
ν_9	γC_4H(28)+γC_5H(25)+γC_6H(18) [(e)]	750.6	52	888.9	98.4	0.8	875.1	114.2	0.4	701.3	101.0
ν_{10}	$\delta_3(52)+\nu$C–O(28) [(f)]	817.2	0.0	893.9	27.5	16.1	892.2	27.0	16.8	770.2	2.9
ν_{11}	γCO(38)+γC_7H(27)+γC_6H(20)+γC_4H(14)	823.2	20	978.1	0.1	5.6	963.7	0.0	3.9	804.3	0.0
ν_{12}	γCO(32)+γC_7H(30)+γC_5H(28)	881.0	12	1072.6	27.0	1.9	1047.5	17.2	1.7	813.7	26.1
ν_{13}	νC_6–$C_5(30)+\delta_4(30)+\nu C_5$–$C_4(21)$	958.0[d,f]	0.0	1104.7	9.8	27.9	1110.3	6.7	29.4	850.1	0.4
ν_{14}	$\delta_2(47)+\delta_4(46)$	972.5	1.0	1132.1	0.1	0.1	1137.5	0.0	0.1	860.3	0.5
ν_{15}	γC_4H(32)+γC_6H(25)+γC_7H(15)+γC_3H(12)	999.3[f]	5.0	1156.4	0.1	0.1	1137.9	2.3	1.6	1026.5	5.9
ν_{16}	γC_5H(24)+γC_6H(24)+γC_4H(16)	1026.1[f]	8	1179.5	2.0	1.7	1169.4	1.4	0.2	1050.3	2.7
ν_{17}	νC_1–$C_4(16)+\nu C_7$–$C_6(14)+\delta C_5$H(10)+δC_2H(10)	1072.4	10	1185.6	23.8	0.3	1189.7	23.9	1.4	1104.1	19.7
ν_{18}	δOH(37)+νC_3–$C_2(14)+\nu C_4$–$C_3(12)+\nu C_7$–$C_6(10)$	1150.7	38	1227.7	78.9	0.7	1254.7	127.9	0.7	1186.2	208.7
ν_{19}	δC_5H(28)+δC_6H(19)+νC_5–$C_4(12)+\nu C_6$–$C_5(12)$	1168.9	70	1296.9	121.3	0.5	1299.3	58.7	4.5	1225.1	1.4
ν_{20}	δC_7H(22)+δC_4H(22)+δC_3H(18)+δC_6H(11) [(g)]	1176.5	80	1319.6	11.4	4.9	1313.4	13.2	5.9	1229.6	2.4
ν_{21}	νC–O(40)+νC_3–$C_2(16)+\nu C_7$–$C_6(13)$	1261.7[f]	62	1365.4	63.4	3.6	1385.8	80.6	5.9	1280.8	8.5
ν_{22}	νC_4–$C_3(21)+\delta$OH(17)+δC_3H(13) [(h)]	1277.4	–	1398.7	3.7	3.7	1399.6	0.7	1.1	1387.3	2.0
ν_{23}	δC_7H(23)+δC_3H(21)+δC_6H(18)+δC_4H(13) [(i)]	1343.0	31	1520.6	23.4	0.7	1512.5	18.6	0.6	1397.9	25.1
ν_{24}	δC_5H(30)+δC_4H(15)+νC_4–$C_3(12)+\nu C_7$–$C_6(12)$	1472.0	23	1638.8	26.1	0.5	1644.7	20.7	0.7	1508.2	22.8
ν_{25}	δC_6H(21)+$\delta_3(20)+\delta C_4$H(14)+δC_3H(17)	1501.0	54	1678.0	38.2	1.5	1682.1	53.3	1.2	1540.4	26.2
ν_{26}	νC_3–$C_2(36)+\delta_3(12)+\nu C_6$–$C_5(11)+\nu C_5$–$C_4(10)$	1603.0[d,f]	70	1762.1	32.1	0.7	1797.7	36.5	13.2	1627.3	31.2
ν_{27}	νC_5–$C_4(34)+\nu C_7$–$C_6(25)+\delta(28)+\delta_4$(l8)	1610.0[d,f]	–	1784.8	46.6	0.7	1814.3	41.5	12.7	1648.2	12.5
ν_{28}	νC_3–H(66)+νC_4–H(26)	3027.0	–	3346.2	9.4	49.0	3347.0	12.4	55.8	3165.5	12.2
ν_{29}	νC_5–H(58)+νC_3–H(23)+νC_4–H(13)	3049.0	–	3360.0	0.7	85.8	3362.2	1.5	87.9	3184.7	0.3
ν_{30}	νC_4–H(57)+νC_5–H(21)	3074.5[e]	–	3369.5	20.9	53.8	3373.5	30.0	61.4	3195.4	23.4
ν_{31}	νC_6–H(74)+νC_5–H(13)	3070.0[f]		3387.0	15.4	116.6	3390.5	24.4	124.8	3210.9	22.9
ν_{32}	νC_7–H(91)	3086.6[e]	–	3403.7	2.5	144.7	3406.8	5.1	166.8	3221.1	6.7
ν_{33}	νO–H(100)	3656.7[e]	50	3916.1	53.2	35.8	4047.8	68.2	33.9	3643.8	31.1

Table 3 (Continued)

Mode	Approximate description[a]	Exp[c]		3–21G/SCF			6–31G/SCF			6–31G/MP2	
	(PED)[b]	ν	A	ν	A	R.a.	ν	A	R.a.	ν	A
H_2O											
ν_{34}	δHOH(100)	1589.1[g]	–	1799.6	79.9	11.5	1737.6	122.9	10.6	1666.3	92.3
ν_{35}	ν^{sym}(O–H)(61)+ν^{asym}(O–H)(38) [(j)]	3638.0[g]	–	3814.0	0.0	95.6	3992.9	2.9	89.9	3651.1	3.8
ν_{36}	ν^{asym}(O–H)(61)+ν^{sym}(O–H)(38) [(k)]	3734.3[g]		3947.5	9.2	44.1	4149.5	54.1	40.1	3829.0	8.4

[a] Abbreviations: ν, stretching; δ, δ_1, δ_2, δ_3 and δ_4 in plane bendings, δ_1 is $\delta(C_4C_3C_2)$, δ_2 is $\delta(C_5C_4C_3)$, δ_3 is $\delta(C_6C_5C_4)$, and δ_4 is $\delta(C_7C_6C_5)$; γ, out-of-plane bending; τ, τ_1, τ_2, τ_3 and τ_4, torsions; τ_1 is $\tau(C_4C_3C_2O_1)$, τ_2 is $\tau(C_5C_4C_3O_2)$, τ_3 is $\tau(C_6C_5C_4O_3)$ and τ_4 is $\tau(C_7C_6C_5O_4)$.

[b] PEDs elements lower than 10% are not included. PEDs elements obtained with 6–31G/SCF are given in the Table 3. Different PEDs obtained with the MP2 method are indicated in the end of the second column:

[(a)] $\tau_3(58)+\tau_1(28)+\tau_2(19)$;

[(b)] $\tau_3(32)+\tau_2(26)+\gamma$CO(40);

[(c)] $\delta_1(47)+\delta_2(24)+\nu$C–O(15);

[(d)] $\delta_2(92)$;

[(e)] $\gamma C_3H(46)+\gamma C_5H(20)+\gamma C_4H(14)+\gamma C_7H(13)$;

[(f)] $\gamma C_3H(45)+\gamma C_7H(27)+\gamma C_5H(12)+\gamma C_6H(10)$;

[(g)] $\delta C_4H(35)+\delta C_3H(21)+\delta C_5H(19)$;

[(h)] νC_7–$C_6(22)+\nu C_4$–$C_3(20)+\delta C_3H(15)+\nu C_6$–$C_5(12)$;

[(i)] $\delta C_6H(22)+\delta OH(18)+\delta C_4H(13)+\nu C_3$–$C_2(11)$;

[(j)] ν^{sym}(O–H)(59)+ν^{asym}(O–H)(41);

[(k)] ν^{asym}(O–H)(59)+ν^{sym}(O–H)(41).

[c] The experimental frequencies for PhOH are taken from Ref.[30], otherwise as indicated:

[d] Ref. [31];

[e] Ref. [32];

[f] Ref. [33];

[g] Ref. [34].

Table 4
Calculated vibrational frequencies (ν, cm^{-1}), infrared intensities (A, km mol^{-1}) and Raman activities (R.a., A^4 amu^{-1}) for the complex $PhOH\cdots H_2O$ at different levels of ab initio MO theory

Mode	Approximate description[a]	3–21G/SCF			6–31G/SCF			6–31G/MP2	
	(PED)[b]	ν	A	Ra	ν	A	Ra	ν	A
ν_1	$\tau(O_{14}O_1C_2C_3)(98)$	34.2	20.1	4.8	36.1	19.9	4.2	40.0	14.8
ν_2	$\delta(O_{14}O_1C_2)(41)$	58.4	23.2	9.8	59.2	8.6	0.0	66.1	12.8
ν_3	$\tau(H_{15}O_{14}O_1C_2)(100)$	77.4	2.8	0.5	115.7	4.1	0.8	70.6	6.0
ν_4	$\nu(O\cdots H)(96)$	177.5	8.9	0.0	183.3	4.2	0.0	189.3	5.7
ν_5	$\tau(H_{16}O_{14}O_1C_{15})(100)$	217.6	7.7	0.1	212.1	7.2	6.9	222.3	6.1
ν_6	$\delta(H_{15}O_{14}O_1)(40)+\delta(H_{16}O_{14}O_1)(40)$	268.9	0.8	3.0	264.6	0.1	2.5	240.2	28.5
ν_7	$\tau_1(65)+\tau_3(30)$ [a]	309.3	59.3	2.5	304.1	64.8	1.9	330.1	56.7
ν_8	$\tau_3(44)+\tau_4(44)$	484.2	0.1	0.0	476.3	0.1	0.0	398.4	1.1
ν_9	$\delta CO(61)+\delta_1(29)+\delta(O_{14}O_1C_2)(10)$	488.6	9.1	0.9	479.9	14.8	0.5	414.0	12.2
ν_{10}	$\tau_3(83)+\gamma C_6H(10)$ [b]	591.9	9.9	0.0	577.2	4.7	0.1	449.8	19.0
ν_{11}	$\delta_1(45)+\delta_2(13)+\nu C–O(11)$	596.7	0.7	6.4	589.9	0.8	4.9	483.3	0.0
ν_{12}	$\delta_2(92)$ [c]	710.4	0.6	4.5	702.2	0.5	4.9	540.9	0.5
ν_{13}	$\tau(H_8O_1C_2C_3)(97)$	807.4	2.5	0.5	741.9	6.1	2.0	642.5	0.5
ν_{14}	$\tau_2(71)+\gamma C_5H(18)$[d]	824.7	82.2	1.4	791.5	51.4	0.0	696.4	0.8
ν_{15}	$\gamma C_4H(26)+\gamma C_5H(26)+\tau_2(24)+\gamma C_6H(18)$ [e]	893.9	135.9	0.7	873.7	131.5	0.3	707.5	404.5
ν_{16}	$\delta_3(52)+\nu C–O(26)$ [f]	897.3	19.3	17.4	899.6	20.8	17.8	774.3	12.9
ν_{17}	$\gamma CO(37)+\gamma C_7H(28)+\gamma C_6H(20)+\gamma C_4H(15)$	977.2	5.1	6.1	963.7	2.1	4.2	797.0	0.6
ν_{18}	$\gamma CO(32)+\gamma C_7H(30)+\gamma C_5H(29)$	1065.8	43.4	1.9	1041.6	24.6	1.8	821.6	19.4
ν_{19}	$\delta_4(34)+\delta_2(28)+\nu C_6–C_5(27)+\nu C_5–C_4(20)$	1104.9	9.9	28.4	1109.5	7.4	29.9	842.4	0.1
ν_{20}	$\delta_2(42)+\delta_4(45)$	1129.9	0.1	0.3	1134.1	0.0	0.2	854.9	0.2
ν_{21}	$\gamma C_4H(32)+\gamma C_6H(24)+\gamma C_7H(14)+\gamma C_3H(13)$	1153.5	0.1	0.2	1137.0	1.6	2.1	1026.6	6.5
ν_{22}	$\gamma C_6H(25)+\gamma C_5H(22)+\gamma C_4H(16)+\tau_4(14)$	1180.3	5.8	0.6	1163.1	1.9	0.3	1050.2	1.7
ν_{23}	$\nu C_4–C_3(19)+\nu C_7–C_6(17)+\delta C_5H(10)+\delta C_2H(10)$	1186.2	4.7	2.1	1193.5	7.2	1.6	1106.9	6.8
ν_{24}	$\delta OH(35)+\nu C_3–C_2(18)+\nu C_4–C_3(14)+\nu C_7–C_6(11)$	1247.9	28.6	1.8	1278.3	21.8	2.6	1220.9	17.9
ν_{25}	$\delta C_7H(21)+\delta C_3H(19)+\delta C_4H(18)+\delta C_6H(17)$ [g]	1316.6	8.4	5.0	1311.0	6.1	6.1	1227.3	7.0
ν_{26}	$\delta C_5H(18)+\delta C_6H(17)+\delta OH(14)+\delta_1(13)$ [h]	1338.7	34.1	2.1	1346.9	109.8	1.4	1258.3	196.1
ν_{27}	$\nu C–O(43)+\nu C_7–C_6(13)+\nu C_3–C_2(10)$	1392.3	179.4	7.1	1400.3	139.5	6.7	1323.7	15.2
ν_{28}	$\delta OH(29)+\delta C_3H(28)+\nu C_4–C_3(15)$ [i]	1456.0	21.5	1.1	1444.4	34.4	1.1	1408.2	4.2
ν_{29}	$\delta OH(32)+\delta C_6H(21)+\delta C_4H(11)+\delta C_5H(10)$	1561.3	93.1	0.7	1535.0	81.1	0.6	1441.8	84.1
ν_{30}	$\delta C_5H(27)+\delta C_4H(15)+\nu C_7–C_6(11)+\nu C_4–C_3(11)$	1646.7	95.3	0.5	1647.9	53.9	0.6	1514.1	74.3
ν_{31}	$\delta C_6H(20)+\delta_3(18)+\delta C_3H(18)+\delta C_4H(12)$	1688.5	7.5	2.5	1687.1	33.4	1.5	1551.8	3.7
ν_{32}	$\delta(H_{15}O_{14}O_1)(41)+\delta(H_{16}O_{14}O_1)(41)$	1757.7	58.6	14.9	1754.1	88.5	11.1	1625.7	48.4
ν_{33}	$\nu C_3–C_2(35)+\delta_4(18)+\delta_3(13)+\nu C_5–C_4(10)$	1780.8	48.9	13.6	1799.7	47.1	14.1	1656.7	44.8
ν_{34}	$\nu C_5–C_4(31)+\delta_1(27)+\nu C_7–C_6(24)+\delta C_7H(19)+\delta_4(16)$	1792.0	91.4	13.5	1816.4	50.4	14.4	1682.6	102.6
ν_{35}	$\nu C_4–H(66)+\nu C_5–H(24)$	3347.8	3.6	42.5	3349.0	4.4	40.7	3171.4	5.8
ν_{36}	$\nu C_6–H(52)+\nu C_5–H(24)+\nu C_4–H(13)+\nu C_7–H(10)$	3357.1	10.9	99.9	3359.6	7.6	118.5	3181.1	3.6
ν_{37}	$\nu C_5–H(39)+\nu C_6–H(35)+\nu C_3–H(22)$	3374.8	35.7	28.3	3371.6	45.7	35.3	3191.7	39.2
ν_{38}	$\nu C_3–H(64)+\nu C_4–H(14)+\nu C_5–H(12)$	3384.3	16.8	147.8	3385.7	28.8	144.8	3205.5	30.1
ν_{39}	$\nu C_7–H(100)$	3400.0	4.0	154.0	3402.0	7.3	174.2	3216.4	9.0
ν_{40}	$\nu O–H(100)$	3620.5	977.7	169.2	3847.9	677.0	149.9	3457.8	666.5

Table 4 (Continued)

Mode	Approximate description[a]	3–21G/SCF			6–31G/SCF			6–31G/MP2	
	(PED)[b]	ν	A	Ra	ν	A	Ra	ν	A
ν_{41}	νH_{15}–O_{14}(58)+νH_{16}–O_{14}(40) [(j)]	3859.7	12.3	101.0	4003.8	17.2	86.8	3655.7	2.8
ν_{42}	νH_{16}–O_{14}(58)+νH_{15}–O_{14}(4) [(k)]	3991.8	68.9	60.4	4152.5	110.4	50.0	3827.9	64.8

[a] Abbreviations: ν, stretching; δ, δ_1, δ_2, δ_3 and δ_4 in plane bendings, δ_1 is $\delta(C_4C_3C_2)$, δ_2 is $\delta(C_5C_4C_3)$, δ_3 is $\delta(C_6C_5C_4)$, and δ_4 is $\delta(C_7C_6C_5)$; γ, out-of-plane bending; τ, τ_1, τ_2, τ_3 and τ_4, torsions; τ_1 is $\tau(C_4C_3C_2O_1)$, τ_2 is $\tau(C_5C_4C_3C_2)$, τ_3 is $\tau(C_6C_5C_4C_3)$ and τ_4 is $\tau(C_7C_6C_5C_4)$.

[b] PEDs elements lower than 10% are not included. PEDs elements obtained with 6–31G/SCF are given in the Table 4. Different PEDs obtained with the MP2 method are indicated in the end of the second column:

(a) $\tau_3(48)+\tau_1(31)+\tau_2(22)$;
(b) $\tau_3(52)+\gamma CO(25)+\tau_2(16)$;
(c) $\delta_1(44)+\delta_3(14)+\nu C$–O(15);
(d) $\delta_2(94)$;
(e) $\gamma C_3H(26)+\gamma C_5H(18)+\gamma C_4H(12)+\gamma C_7H(10)$;
(f) $\gamma C_3H(46)+\gamma C_5H(19)+\gamma C_7H(14)$;
(g) $\delta C_4H(38)+\delta C_5H(23)+\delta C_3H(17)$;
(h) $\nu CO(38)+\delta_1(20)+\delta_3(20)+\nu C_4$–$C_3(13)$;
(i) νC_7–$C_6(22)+\nu C_4$–$C_3(19)+\delta C_3H(14)$;
(j) νH_{15}–$O_{14}(75)+\nu H_{16}$–$O_{14}(24)$;
(k) νH_{16}–$O_{14}(75)+\nu H_{15}$–$O_{14}(24)$.

from monomers to a complex, in our study the 'optimal' scale factors for the stretching, bending and torsion vibrations are used. The 'optimal' scale factors of the monomers are determined using the ratio ν^{exp}/ν^{calc}. The concept of the 'optimal' scale factor has been proposed by Destexhe et al. [39] in order to obtained an estimation of the anharmonicity of the modes in H-bonded H_2O with pyridine. This procedure could only be applied for modes which are experimentally accessible in the spectral region.

The shifts in the vibrational frequencies ($\Delta\nu^{scal}$) of phenol and water upon formation of the hydrogen-bonded complex have been calculated at different levels of ab initio MO theory: 3–21G/SCF, 6–31G/SCF and 6–31G/MP2 by using the corresponding scale factors. For each vibration the predicted frequency shift is:

$$\Delta\nu^{scal} = k_i(\nu_i^{complex} - \nu_i^{monomer}),$$

where k_i is the corresponding 'optimal' scale factor.

The 'optimal' scale factor for the stretching OH vibration for free phenol at the SCF level is smaller than the corresponding scale factor for the complex. This is connected to the increase of anharmonicity of the bonded OH group of phenol by the H-bond interaction.

The changes in the vibrational frequencies $\Delta\nu$, infrared intensities ΔA and Raman activities ΔR.a. from free to complexed PhOH and H_2O are shown in Table 5.

In our previous studies [15–17] it was established that the stretching vibrations of the monomer bonds, involved in the hydrogen bonding are most sensitive to the complexation. For the complex studied here (see Fig. 1) these vibrations are: the stretching O–H vibration (ν_{33}) of phenol and the symmetric and asymmetric O–H vibrations (modes ν_{35} and ν_{36}) of water.

The O–H stretching vibration ν_{OH} of free phenol (see Table 3, mode ν_{33}) is predicted at the 6–31G/MP2 level at 3643.8 cm^{-1} with medium IR intensity. In agreement with the experiment [12], for the complex of phenol with one water molecule PhOH···H_2O, the O–H band is shifted to lower wavenumbers. The predicted frequency shift with the 3–21G/SCF basis set is -274.3 cm^{-1}, with the 6–31G/SCF basis set is -180.5 cm^{-1} and with the G–31G/MP2 is -186.0 cm^{-1}.

Table 5
Changes in the vibrational frequencies $\Delta\nu$ (in cm^{-1}), infrared intensities ΔA (in km mol^{-1}) and Raman activities $\Delta R.a.$ (in A^4 amu^{-1}) from monomers to the complex $PhOH\cdots H_2O$ calculated at different levels of ab initio MO theory: 3–21G/SCF, 6–31G/SCF and 6–31G/MP2

Monomer mode	Dimer mode	3–21G/SCF			6–31G/SCF			6–31G/MP2	
		$\Delta\nu^{unscal}/\Delta\nu^{scal}$	ΔA	$\Delta R.a.$	$\Delta\nu^{unscal}/\Delta\nu^{scal}$	ΔA	$\Delta R.a.$	$\Delta\nu^{unscal}/\Delta\nu^{scal}$	ΔA
ν_1	ν_7	44.0/40.5	50.9	0.6	42.6/39.6	60.7	−0.3	107.4/117.1	56.6
ν_3	ν_9	61.7/58.2	−4.4	0.3	48.1/45.1	0.1	0.0	19.4/19.8	−0.9
ν_4	ν_8	1.6/1.3	0.0	0.0	0.9/0.8	0.0	0.0	−1.1/−1.1	0.5
ν_5	ν_{10}	3.6/3.1	2.7	0.0	2.4/2.1	−3.1	0.1	18.2/21.1	17.2
ν_6	ν_{11}	6.1/5.4	−1.8	1.2	4.7/4.2	−2.1	4.4	0.2/0.2	−0.6
ν_7	ν_{12}	0.5/0.4	0.4	0.2	0.6/0.5	0.2	0.1	5.9/6.8	−2.1
ν_8	ν_{14}	17.3/14.1	−40.4	1.3	2.1/1.8	25.7	0.0	54.7/58.5	0.5
ν_9	ν_{15}	5.0/4.2	37.5	−0.1	−1.4/−1.2	17.3	−0.1	6.2/6.6	303.5
ν_{10}	ν_{16}	3.4/3.1	−8.2	1.3	7.4/6.8	−6.2	1.0	4.1/4.3	10.3
ν_{11}	ν_{17}	−0.9/−0.7	5.0	0.5	0.0	2.1	0.3	−7.3/−7.4	0.6
ν_{12}	ν_{18}	−6.8/−5.6	16.4	0.0	−5.9/−5.0	7.4	0.1	7.9/8.5	−6.7
ν_{13}	ν_{19}	0.2/0.2	0.1	0.5	−0.8/−0.7	0.7	0.5	−7.7/−8.6	−0.3
ν_{14}	ν_{20}	−2.2/−1.9	0.0	0.2	−3.4/−2.9	0.0	0.1	−5.4/−6.1	−0.3
ν_{15}	ν_{21}	−2.9/−2.5	0.0	0.1	−0.9/−0.8	−0.7	0.5	0.1/0.1	0.6
ν_{16}	ν_{22}	0.8/0.7	3.8	−1.1	−6.3/−5.5	0.5	0.1	−0.1/−0.1	−1.0
ν_{17}	ν_{23}	0.6/0.5	0.9	−19.1	3.8/3.4	−16.7	0.2	2.8/2.7	−12.9
ν_{18}	ν_{24}	62.3/58.3	4.8	1.5	88.6/81.2	−2.1	1.2	116.8/113.3	−1.8
ν_{20}	ν_{25}	−3.0/−2.6	−3.0	0.1	−2.4/−2.1	−7.1	0.2	−2.3/−2.2	4.6
ν_{21}	ν_{27}	26.9/24.8	116.0	3.5	14.2/12.9	58.9	0.8	42.9/42.0	6.7
ν_{22}	ν_{28}	57.3/52.3	17.8	−2.6	44.8/40.9	0.4	0.0	20.9/20.5	2.2
ν_{24}	ν_{30}	7.9/7.0	69.2	0.0	3.2/2.8	33.2	−0.1	5.9/5.4	51.5
ν_{25}	ν_{31}	10.5/9.4	−30.7	1.0	5.0/4.5	−19.9	0.3	11.4/11.1	−22.5
ν_{26}	ν_{33}	18.7/17.0	16.8	12.9	2.0/1.8	10.6	0.9	29.4/28.8	13.6
ν_{27}	ν_{34}	7.2/6.5	44.8	12.8	2.1/1.7	8.9	1.7	34.4/33.7	90.1
ν_{28}	ν_{38}	38.1/34.5	7.4	98.8	38.7/35.0	16.4	89.0	40.0/38.4	17.9
ν_{29}	ν_{37}	14.8/13.4	35.0	−57.5	9.4/8.5	44.2	−52.6	7.0/6.7	38.9
ν_{30}	ν_{35}	−21.5/−19.1	−17.3	−11.3	−24.5/−22.3	−25.6	−20.7	−24.0/−23.0	17.6
ν_{31}	ν_{36}	−29.9/−27.1	−4.5	−16.7	−30.9/−28.0	−16.8	−6.3	−29.8/−28.6	−19.3
ν_{32}	ν_{39}	−3.7/−3.3	1.5	9.3	−4.8/−4.3	2.2	7.4	−4.7/−4.5	2.3
ν_{33}	ν_{40}	−295.6/	924.5	168.9	−199.9/	608.8	46.0	−186.0/	635.4
		−274.3			−180.5			−186.0	
ν_{35}	ν_{41}	45.7/43.6	12.3	5.4	10.9/9.9	14.3	−3.1	4.6/4.5	−1.0
ν_{36}	ν_{42}	44.3/41.9	59.7	16.3	3.0/2.7	56.3	9.9	−1.1/−1.1	56.4

The experimentally observed red shift for the O–H stretching vibration in $PhOH\cdots H_2O$ is 133 cm^{-1}. The ab initio calculations at different levels overestimate the magnitude of the experimentally measured red shift. The magnitude of the wavenumber shift is indicative of relatively strong OH···H hydrogen-bonded interaction. The calculated values of the binding energy with various basis sets, corrected for the basis set superposition errors (BSSE) and MP2 correlation contribution for the complex $PhOH\cdots H_2O$ (planar structure) confirm also relatively strong hydrogen-bonded interaction (see Table 6).

As a result of the hydrogen bonding the IR

intensity and Raman activity of the stretching OH vibration of phenol increase significantly. As can be seen from he results in Table 5, the ab initio calculations at different levels predict an increase of the IR intensity to 50 times and of the Raman activity to four times.

The stretching O–H vibrations for free water molecule (see Table 3, modes ν_{35} and ν_{36}) appear at 3638.0–3734.3 cm^{-1} [34]. The ab initio calculations at the 6–31G/MP2 level predict the stretching O–H vibrations of water at 3651–3829.0 cm^{-1} with low IR intensity and medium Raman activity.

As can be seen from the results in Table 4, the ν_{41}, and ν_{42} vibrations of PhOH···H_2O are very close to the corresponding vibrations of pure H_2O, although they are slightly shifted by only a few wavenumbers (Table 5). In the same time the IR intensity of the modes ν_{41} and ν_{42} increases significantly in the complex to seven times, while the Raman activity of the same modes increases by about 20%.

The data for the changes of the vibrational characteristics of the stretching OH vibration of the phenol site and of the O–H stretching vibrations of the water side indicate that the force field of the O–H bond of PhOH is substantially reduced by the hydrogen bonding, but only a little change of the force field occurs in the O–H bonds of the proton accepting H_2O site.

The remaining vibrations (stretching, bending and torsion) are less sensitive to the complexation. Their vibrational characteristics are changed to a smaller extent.

Table 6
Ab initio calculated total energy in a.u. and binding energy ΔE (uncorrected and corrected), basis set superposition error (BSSE) and MP2 correlation contribution δE(MP2) in cm^{-1} for free and complexed PhOH and H_2O

	6–31G**/SCF	6–31G**/MP2	DZP/SCF
H_2O	−76.023615	−76.222449	−76.046861
PhOH	−305.573753	−306.575492	−305.623614
PhOH···H_2O	−381.607594	−382 809981	−381.690055
ΔE (uncorr)	−2244.2	−2643.6	−2102.6
ΔE (corr)	−2011.9	−2179.8	−2004.9
BSSE	232.2	463.8	97.7
δE(MP2)	–	−399.4	–

3. Conclusions

In the present study the changes in the vibrational characteristics (vibrational frequencies, infrared intensities and Raman activities) upon hydrogen bonding for the hydrogen-bonded complex PhOH···H_2O have been investigated using ab initio calculations at different levels of ab initio MO theory: 3–21G/SCF, 6–31G/SCF and 6–31G/MP2. The main results of the present study are as follows:

1. The complexation between PhOH and H_2O leads to changes in the geometric parameters of the monomers. The most sensitive to the formation of the hydrogen bond is the hydrogen-bonded OH bond (H_8O_1) and the angle $H_8O_1C_2$. The remaining geometric parameters of the monomers are either unchanged or changed with small values upon formation of the hydrogen bond.
2. The changes of the atomic charges (Δq_i) from monomers (PhOH and H_2O) to a complex PhOH···H_2O show that as a result of the hydrogen bonding between PhOH and H_2O a charge rearrangement occurs.
3. The most sensitive to the complexation is the stretching O–H vibration of the phenol site. In agreement with the experiment its vibrational frequency is shifted to lower wavenumbers. The magnitude of the wavenumber shift is indicative of relatively strong OH· · · H hydrogen-bonded interaction. The ab initio calculations at different levels predict an increase of the IR intensity to 50 times and of the Raman activity to four times.
4. The remaining vibrations (stretching, bending and torsion) are less sensitive to the complexation. Their vibrational characteristics are changed with smaller magnitude.

Acknowledgements

The research was supported by the Royal Society (UK). This financial support is gratefully acknowledged. The author would like to thank Professor David C. Clary, FRS for many useful suggestions and the University College London for the use of their computing facilities.

References

[1] R.J. Stanley, A.W. Castleman, J. Chem. Phys. 94 (1991) 7744.
[2] T. Ebata, M. Furukawa, T. Suzuki, M. Ito, J. Opt. Soc. Am. B7 (1990) 1890.
[3] M. Schütz, T. Bürgi, T. Fisher, J. Chem. Phys. 98 (1993) 3763.
[4] M. Schmitt, U. Henrichs, H. Müller, K. Kleinermanns, J. Chem. Phys. 103 (1995) 9918.
[5] R.J. Lipert, S.D. Colson, J. Chem. Phys. 94 (1989) 2358.
[6] G.V. Hartland, B.F. Henson, V.A. Venturo, P.M. Felker, J. Phys. Chem. 96 (1992) 1164.
[7] A. Schiefke, C. Deusen, C. Jacoby, M. Gerhards, M. Schmitt, K. Kleinermanns, P. Hering, J. Chem. Phys. 102 (1995) 9197.
[8] M. Schutz, T. Burgi, S. Leutwyler, J. Mol. Struct.(Theochem) 276 (1992) 117.
[9] D. Feller, M.W. Feyereisen, J. Comput. Chem. 14 (1993) 1027.
[10] M. Gerhards, K. Beckman, K. Kleinermanns, Z. Phys. D29 (1994) 224.
[11] S. Tanabe, T. Ebata, M. Fujii, N. Mikami, Chem. Phys. Lett. 215 (1993) 347.
[12] N. Mikami, Bul. Chem. Soc. Jpn. 68 (1995) 683.
[13] T. Bürgi, M. Schütz, S. Leutwyler, J. Chem. Phys. 103 (1995) 6350.
[14] M. Gerhards, K. Kleinermanns, J. Chem. Phys. 103 (1995) 7392.
[15] Y. Dimitrova, J. Mol. Struct.(Theochem) 391 (1997) 251.
[16] Y. Dimitrova, Spectrochim. Acta, Part A (in press).
[17] Y. Dimitrova, B.A. Stamboliyska, Spectrochim. Acta, Part A (in press).
[18] Y. Dimitrova, J. Mol. Struct. (Theochem) 1998 (in press).
[19] X.Q. Lewell, I.H. Hillier, M.J. Field, J.J. Morris, P.J. Taylor, J. Chem. Soc. Faraday Trans. 2 (84) (1988) 893.
[20] G.A. Yeo, T.A. Ford, Theor. Chim. Acta 81 (1992) 255.
[21] M. Pohl, M. Smchimitt, K. Kleinermanns, J. Chem. Phys. 94 (1991) 1211.
[22] M. Pohl, M. Smchimitt, K. Kleinermanns, Chem. Phys. Lett. 177 (1991)
[23] M. Schütz, T. Bürgi, S. Leutwyler, T. Fischer, J. Chem. Phys. 98 (1993) 3763.
[24] M. Schütz, T. Bürgi, S. Leutwyler, T. Fischer, J. Chem. Phys. 99 (1993) 1847.
[25] M. Schütz, T. Bürgi, S. Leutwyler, Theochem 276 (1992) 117.
[26] M. Pohl, K. Kleinermanns, Z. Phys. D 8 (1988) 385.
[27] M. Gerhards, K. Beckmann, K. Kleinermanns, Z. Phys. D 29 (1994) 231.
[28] P. Hobza, R. Burcl, V. Spirko, O. Dopfer, K. Muller-Dethlefs, E. Schlag, J. Chem. Phys. 101 (1994) 990.
[29] D. Feller, M.W. Feyereisen, J. Comp. Chem. 14 (1993) 1027.
[30] H.D. Bist, J.S.D. Brand, D.R. Williams, J. Mol. Spectrosc. 24 (1967) 402.
[31] J.C. Evans, Spectrochim. Acta 16 (1960) 1382.
[32] J.H.S. Green, D.J. Harrison, W. Kynaston, Spectrochim. Acta 27A (1971) 2199.
[33] G.V. Hartland, B.F. Henson, V.A. Venturo, P.M. Felker, J. Phys. Chem. 96 (1992) 1164.
[34] B. Nelander, J. Chem. Phys. 72 (1980) 771.
[35] G. Chatasinski, M.N. Szczesniak, Chem. Rev. 94 (1994) 1723.
[36] M.K. Van Bael, J. Smets, K. Schoone, L. Houben, W. McCarthy, L. Adamowicz, M.J. Nowak, G. Maes, J. Phys. Chem. 101 (1997) 2397.
[37] H. Seller, P. Pulay, J.E. Boggs, J. Am. Chem. Soc. 107 (1985) 6487.
[38] G. Fogarasi, P. Pulay, in: J.R. During (Ed.), Vibrational spectra and structure, vol. 14, Elsevier, Amsterdam, 1985.
[39] A. Destexhe, J. Smets, L. Adamowicz, G. Maes, J. Phys. Chem. 98 (1994) 1506.
[40] T. Pedersen, N.W. Lasen, L. Nygaard, J. Mol. Struct. 4 (1969) 50.
[41] W.L. Jordensen, J. Chandrasekhar, J.D. Madura, R.W. Imprey, M. Klein, J. Chem. Phys. 79 (1983) 926.